avidity は高く、高濃度のフィブリノーゲント共存在下でも血小板と結合することが可能である。実際に経静脈投与により血小板減少症マウスの出血時間の短縮が認められているが、臨床応用を考慮した場合、製剤の機能の安定性が確保されていなければならない。すなわち、製剤間の機能のばらつきを最小限にとどめなくてはならない。そのためには、H12-vesicle の機能を評価する測定系の確立が不可欠である。

H12-vesicle の機能の測定法には幾つかの方法が考えられるが、それぞれ問題点を抱えている。1）血小板と H12-vesicle の結合を測定：この場合、H12-vesicle を蛍光色素あるいは放射性アイソトープで標識し、血小板と混和した後に、結合した H12-vesicle 量を FACS あるいは放射線測定機器で測定する。この過程で H12-vesicle を化学修飾することになるため、H12-vesicle の機能が影響を受ける可能性がある。しかし DiOC18 などの蛍光色素は脂質膜成分に結合するため、αIIbβ3 結合部位である H12-ペプチド部分への影響は少ないと考えられる。また、前述したように血小板が H12-vesicle と結合するためには、活性化なければならない。このためには血小板を ADP、トロンビンなどのアゴニストと反応させる必要がある。ここで最大の問題は、そもそも血小板をヒトから採取する段階で活性化を受ける可能性があることである。また、ADP、トロンビンなどの反応性に個人差があることも大きな問題である。つまり、再現性のある結果を得るためには、特定の個人からの血小板を使い続けなければならず、例えそうでも操作の過程で血小板の機能が影響を受けてしまう危険性が高い。以上から、血小板そのものを用いるのは、測定系として妥当ではないと考えられる。

2）αIIbβ3 発現細胞と H12-vesicle の結合を測定（図 1A）：これまでの研究で、われ

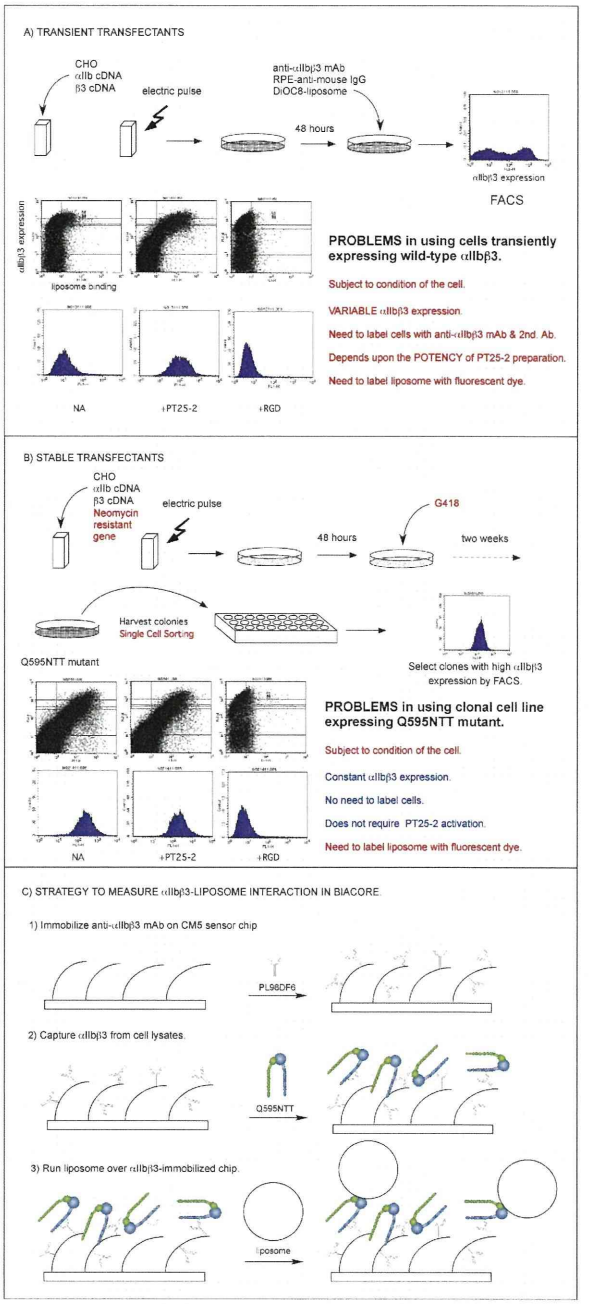

図 1．H12-vesicle の機能測定系

われは CHO 細胞膜表面にαIIb β3 を一過性発現させた細胞を用い、H12-vesicle の機能を検討してきた。ここでも、H12-vesicle を標識する必要があるが、血小板の代わりにαIIbβ3 を発現した動物細胞を用いるため、血小板のように個人差や採取の過程での影響を排除することができる。しかし、CHO 細胞に発現したαIIbβ3 は不活性であるため、H12-vesicle との結

合を調べるためには、活性化モノクローナル抗体PT25-2を用いてαIIbβ3そのものを活性化する必要がある。すなわち、実験結果が使用するPT25-2の活性に依存することとなる。また、一過性発現の系では、αIIbβ3の発現量を正確にコントロールできないため、測定ごとにαIIbβ3の発現量を測定し、補正を加えなくてはならない。

3）αIIbβ3発現細胞株とH12-vesicleの結合を測定（図1B）：測定系は2）と同じであるが、細胞はαIIbβ3を安定発現したクローン細胞を用いるため、測定ごとにαIIbβ3の発現を調べる必要がなく、複数の測定結果の比較も容易となる。この場合もPT25-2を使用する必要があるが、これを回避する方法としては、αIIbβ3のQ595NTT変異体の使用が考えられる。これは、αIIbβ3の高次構造が常にextendedの状態になるようにデザインされたものであり、常に高活性状態にあることが確認されている。この測定系で結果に影響を与える不確定要素は、細胞の状態とH12-vesicleの標識のみであろう。しかし最大の問題は、αIIbβ3を多量に発現した細胞株が得られるか否かである。

4）表面プラスモン共鳴によるαIIbβ3とH12-vesicleの直接結合の測定（図1C）：表面プラスモンセンサー側にαIIbβ3を固層化し、その上にH12-vesicleを流す事によって結合をリアルタイムで測定する。この場合、生きた細胞を使用せず、H12-vesicleの標識も不要であるため、測定に関わる不確定要素をほぼ排除することができる。

本年度の研究では、H12-vesicleの機能の機能評価系として実現性の高い複数の測定法を実施して各方法の問題点を考察するとともに、実際にH12-vesicle製剤のロット間で差が認められるか否かを検討した。

B. 研究方法

I. αIIbβ3変異体の作成

αIIb鎖、β3鎖のcDNAはJoseph C. Loftus博士（Mayor Clinic. AZ）から供与された。これらを哺乳類発現ベクターであるpBJ-1（Mark Davis博士　University of California, San Francisco）から供与）にクローニングした。高活性型αIIb変異体であるQ595NTTのcDNAはsite-directed mutagenesis法を用いて作成した。

II. 細胞培養とトランスフェクション

Chinese hamster ovary（CHO-K1）細胞は10% fetal calf serum、1% penicillin and streptomycin、1% non-essential amino acids添加Dulbecco's modified Eagles mediumを用い37 °C、CO2濃度5%のincubatorで行った。50 μgのαV又はαIIb cDNAは50 μgのβ3 cDNAと一緒にCHO-K1細胞へelectroporation法を用いてトランスフェクトした。一過性発現細胞を用いた実験では、トランスフェクトした細胞は48時間後に培養皿から剥離し解析に用いた。

III. Flow Cytometry

細胞を剥離した後1mM Ca^{2+}/1mM Mg^{2+}加Hepes-Tyrode buffer（HTB）に再浮遊させ、各モノクローナル抗体10μg/mlと混和し氷上で30分間反応させた。遠心洗浄した後、二次抗体としてRPE標識抗マウスIgGと氷上で30分間反応させた。遠心洗浄の後細胞を1mM Ca^{2+}/1mM Mg^{2+}加Hepes-buffered saline（HBS）に再浮遊させ、FACSCaliburを用いて細胞の各モノクローナル抗体による陽性率と蛍光強度を測定した。

IV. αIIbβ3を安定発現したクローン細胞の作成

50 μgのαIIb cDNA、50 μgのβ3 cDNAと共に5 μgのNeomycin resistant gene pFneoをトランスフェクトして48時間培養した後、700 μg/mlのG418を含んだ培養液でさらに2-3週間コロニーが形成されるまで培養した。コロニーを剥離した後、

抗αIIbβ3 抗体、二次抗体として RPE 標識抗マウス IgG と反応させ、single cell sorter にてαIIbβ3 発現量の高い細胞を一個ずつ 96 穴プレートに採取した。700 μg/ml の G418 を含んだ培養液でさらに 2-3 週間培養して細胞を増やした後、αIIbβ3 の発現量を FACS にて測定して発現量の高い細胞を保存した。

V. H12-vesicle *結合実験*

野生型あるいは変異を有するαIIb cDNA 50 μg と野生型β3 cDNA 50 μg を CHO 細胞にトランスフェクトした。 48 時間後細胞を剥離して 10 μg/ml の抗αIIb モノクローナル抗体 PL98DF6 を含有する HTB に再浮遊して氷上で 30 分間反応させた後細胞を遠心洗浄し、RPE 標識抗マウス IgG と氷上で 30 分間反応させた。H12-vesicle とαIIbβ3-CHO との結合は、異なる濃度の DiOC18 標識 H12-vesicle（FH12V）を、10 μg/ml のマウス IgG、PT25-2、あるいは 1mM の GRGDS ペプチドを含んだ HTB と氷上で 2 時間反応させ行った。細胞を 1mM Ca^{2+}/1mM Mg^{2+} 加 HBS に再浮遊させ、FACSCalibur を用いて FL2>500 の領域の細胞集団の平均蛍光強度（FL1）を測定した。各抗体存在下での結合から GRGDS ペプチド存在下での結合をバックグラウンドとして差し引き、特異的結合を算出した。

C. 研究結果

I. DiOC18 標識 H12-vesicle の FACS 解析

前述したように、DiOC18 はリポソームの脂質膜成分に結合する蛍光色素である。その放出する蛍光は緑色であるため、FACS では FITC と同じチャンネル FL-1 で計測可能である。図 2 は製造日時の異なる H12-vesicle 製剤 Lot#903 と Lot#904 を DiOC18 標識し、FACS でその蛍光強度を比較した結果である。左にドットプロット（FSC/SSC）、中央にドットプロット

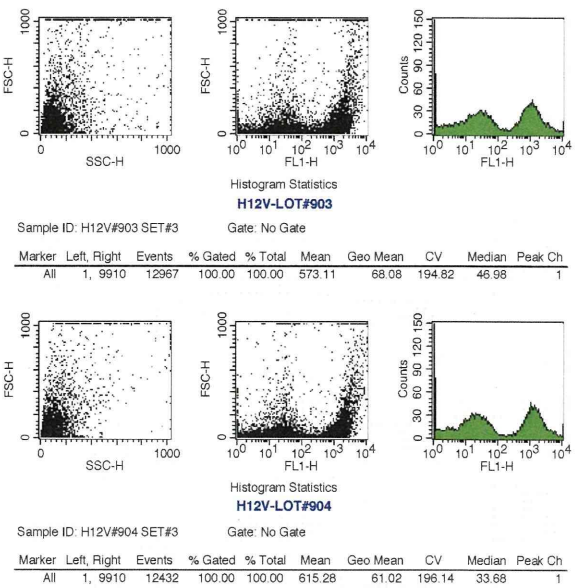

図 2．DiOC18 標識 H12-vesicle の FACS 解析

（FSC/FL1）、右にヒストグラム（FL1）を示す。ドットプロット（FSC/SSC）をみると両粒子の FSC 値はほぼ同じであり、同じ粒子径を有していることがわかる。しかし、ドットプロット（FSC/FL1）をみると、各リポソーム粒子の蛍光強度は均一ではなく、大きく二つの集団に分かれることがわかる。ヒストグラムをみると、両粒子の蛍光強度にはかなりのバラツキがあり、２峰性になっていることが明らかである。しかし、平均蛍光強度（Geo Mean）を見ると、Lot#903 で 68.08、Lot#904 で 61.02 であり、ほぼ同じ値を示していた。

II. H12-vesicle とαIIbβ3-CHO の結合解析：一過性発現細胞を用いた解析

まず、野生型αIIbβ3 を発現した CHO 細胞を用いて測定を行った。H12-vesicle は製造日時の異なる Lot#903 と#904 を使用した。図 3 は蛍光色素 DiOC18 で標識した H12-vesicle とαIIbβ3-CHO 細胞の結合を FACS にて測定したものである。横軸は DiOC18 標識 H12-vesicle 濃度、縦軸は細胞への結合量（平均蛍光強度 MFI）を示す。それぞれ総結合量と結合阻害剤である RGD ペプチド共存在下での非特異的結合

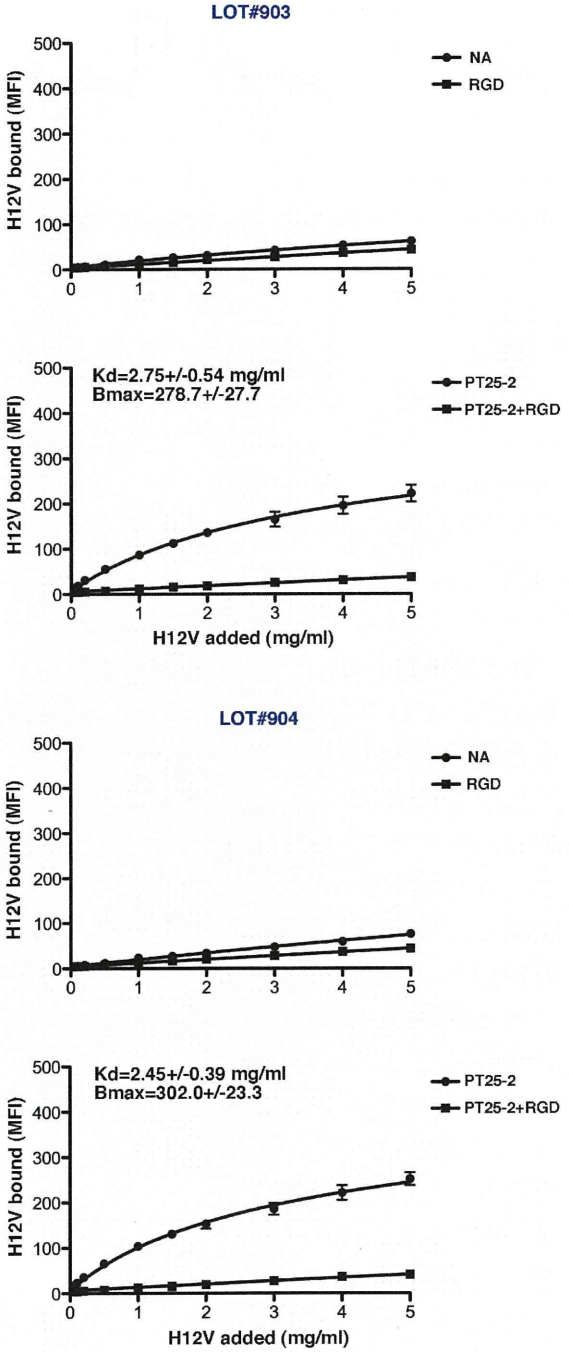

図3．野生型 αIIbβ3-CHO と H12-vesicle の結合

を示した。両 Lot とも活性化抗体である PT25-2 非存在下では、αIIbβ3-CHO と僅かに結合するだけだった。ところが、PT25-2 存在下では容量依存性に結合の増加がみられ、その結合の Kd 値はそれぞれ 2.75±0.54 mg/ml、2.45±0.39 mg/ml 、

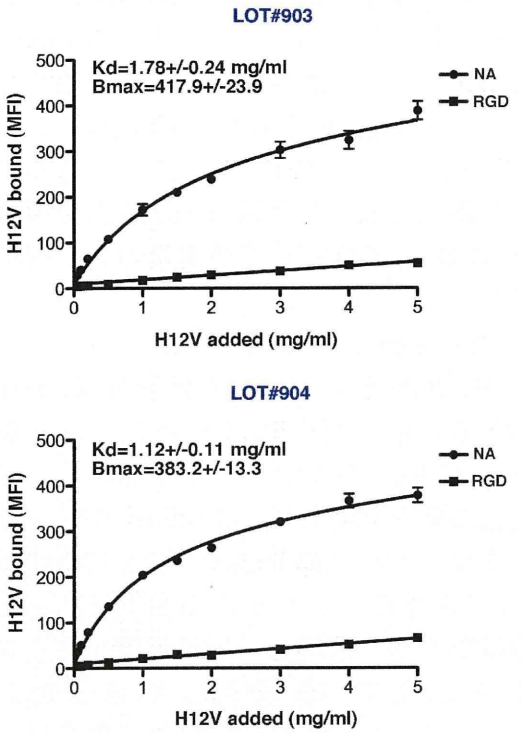

図4．高活性型αIIbβ3（Q595NTT）-CHO と H12-vesicle の結合

Bmax 値はそれぞれ 278.7±27.7 、302.0±23.3 であった。次に、Q595NTT 変異体を発現した細胞を用いて同様の結合実験を行った（図4）。Q595NTT 変異体は高活性型のαIIbβ3 を発現した細胞で、活性化抗体なしでもフィブリノーゲンを結合する。同様に、両 Lot とも PT25-2 非存在下で濃度依存性に Q595NTT 変異体発現細胞と結合した。結合の Kd 値はそれぞれ 1.78±0.24 mg/ml、1.12±0.11 mg/ml 、Bmax 値はそれぞれ 417.9±23.9、383.2±13.3 であった。

次に、H12 ペプチドを担持していないリポソーム粒子についても同様の検討を行った。使用した試料は製造日時の異なる Lot#901 と Lot#902 であり、何れも DiOC18 で標識した。図5に示したように、Lot#901、Lot#902 共に、PT25-2 で活性化した野生型αIIbβ3-CHO と全く結合せず、高活性型の Q595NTT 変異体を発現した細胞とも全く結合しなかった。

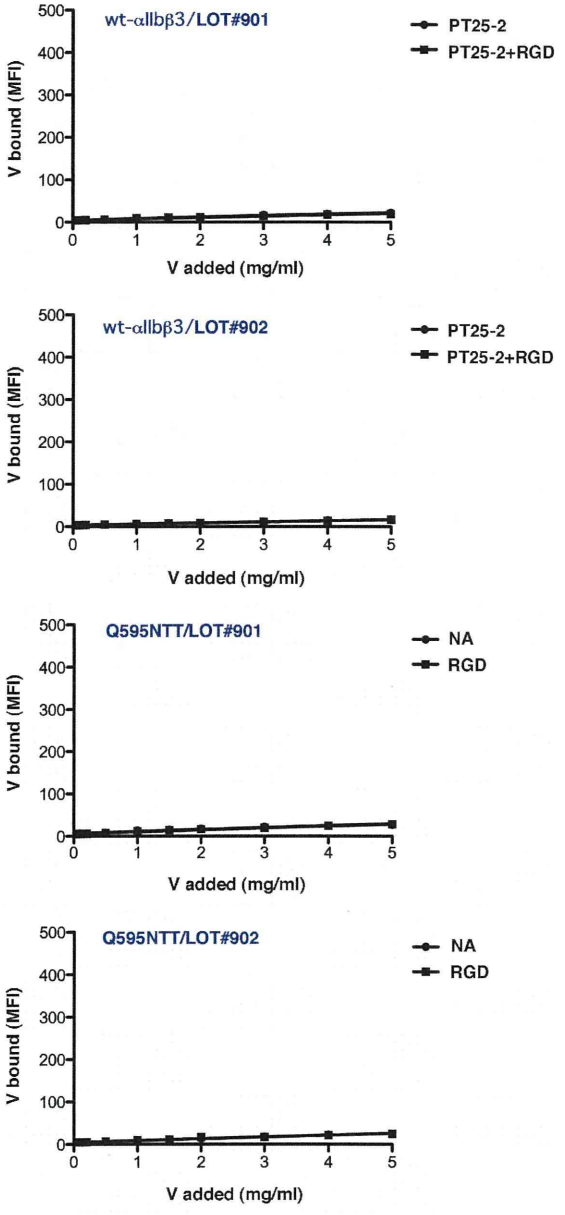

図５．リポソーム vesicle とαIIbβ3-CHO の結合

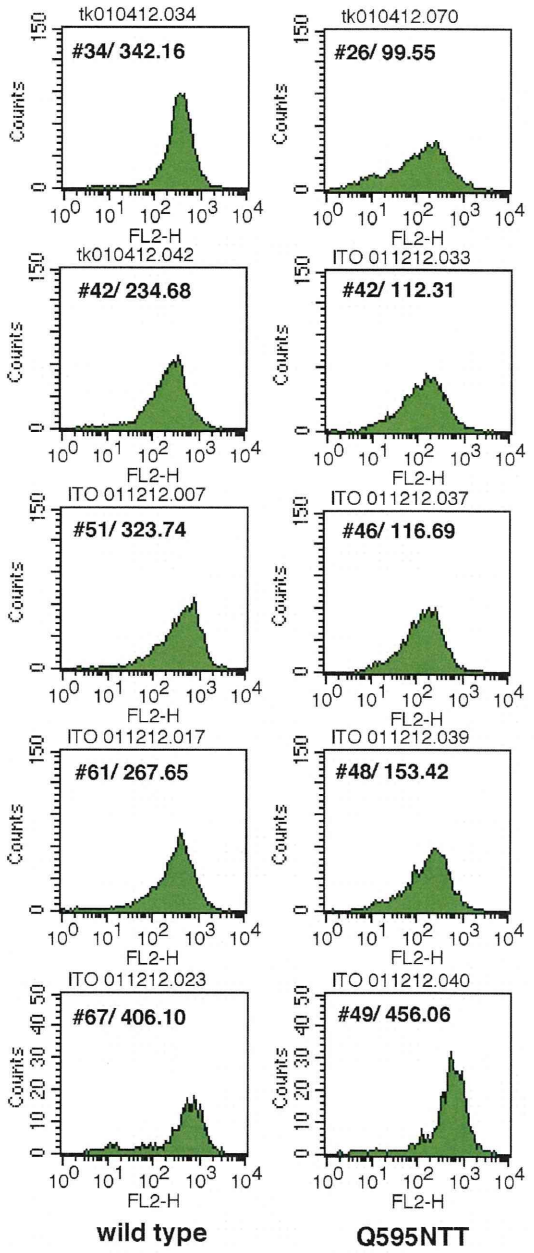

図６． αIIbβ3 安定発現細胞株の FACS 解析

III. H12-vesicle とαIIbβ3-CHO の結合：安定発現細胞を用いた解析

野生型αIIbβ3 と Q595NTT 変異体の安定発現細胞を single cell sorting した結果、幾つかの細胞株を得ることができた。図６にその発現を示す。何れもシングルピークのクローンが得られたが発現は低く、特に Q595NTT クローンの発現は#49 を除き、MFI＜200 であった。Wild type #67 と Q595NTT#49 の発現量はいずれも MFI ＞400 と高かったが、増殖が非常に遅く実際の使用には適さなかった。図７は wild type #51、Q595NTT#48 と H12-vesicle Lot#903、Lot#904 の結合を調べたものである。wild type #51 は PT25-2 存在下での結合を調べた。容量依存性に結合の増加がみられたものの、一過性発現細胞を用いた時と異なり、5 mg/ml でも結合はプラト

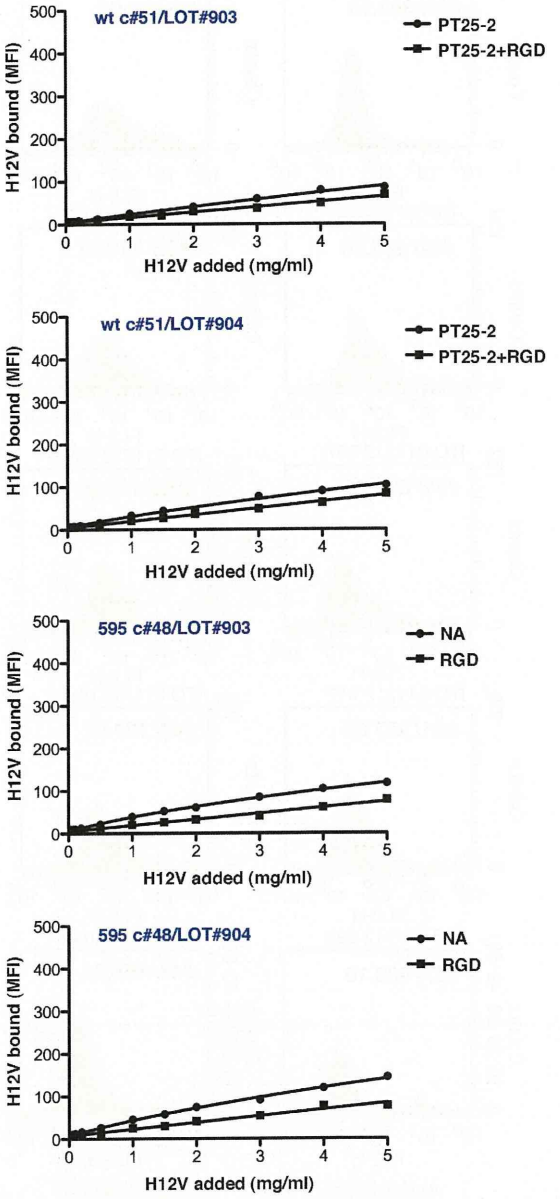

図 7 . αIIbβ3 安定発現細胞株と H12-vesicle の結合

一に達しなかった。同様に、Q595NTT#48 への結合も PT25-2 非存在下で用量依存性に増加したものの、5 mg/ml で飽和傾向を認めず、10 mg/ml の高濃度でも飽和することはなかった（データ記載せず）。

D. 考察

本研究は、１）複数の測定系を用いて H12-vesicle の機能を評価し、どの測定系が最適であるかを見いだすと共に、２）H12-vesicle 製剤の Lot 間での機能の違いを検討することを目的とした。

前述した通り、H12-vesicle 機能測定法には、１）血小板と H12-vesicle の結合測定、２）αIIbβ3 発現細胞と H12-vesicle の結合測定、３）αIIbβ3 と H12-vesicle の直接結合の測定、が考えられる。このうち、１）は一番理に適っているものの、再現性に乏しく、測定法としては適当ではないと考えられる。２）は血小板の代わりにαIIbβ3 を発現した細胞を用いる方法である。Primary cell ではなく、細胞株であることが望ましいが、αIIbβ3 を多量に発現した細胞株は存在しないため、αIIbβ3 遺伝子を人工導入した細胞を用いた。この方法では、一過性発現細胞と安定発現細胞の二つがある。一過性発現系ではαIIbβ3 の発現量は細胞によって異なるが、中には非常に多量に発現した細胞を得ることができる。しかし、この発現は一過性であるため、測定毎に新たに細胞にαIIbβ3 遺伝子を導入しなければならない。また、αIIbβ3 の発現量は毎回異なるため、一定の発現量を持った細胞との結合を調べるためには、毎回αIIbβ3 の発現量を測定し、その値で結合量を補正するなどの手間が必要である。一方、安定発現系は細胞を作成するためにある程度時間が必要である。しかし、一旦作成してしまえば、毎回同一のαIIbβ3 発現量を持った細胞と H12-vesicle の結合を調べることができるため、再現性に優れる。しかし、外来性の遺伝子を多量に発現した細胞は増殖速度が遅いため、実際にはαIIbβ3 を多量に発現した細胞の作成は困難であることが予想される。３）は細胞を用いず、精製したαIIbβ3 と H12-vesicle の直接結合を調べる方法である。これは細胞を使用しないため、最も再現性に優れた方法である。また、H12-vesicle を化学標識する必要がないため、化学修飾による影響を無視できる。し

かし、精製したαIIbβ3をどのようにして得るかが問題となる。

細胞を用いた測定法では、H12-vesicleを化学標識する必要がある。この場合、蛍光標識と放射性アイソトープによる標識が考えられるが、利便性を考慮し蛍光標識を選択した。蛍光標識したH12-vesicleと細胞の結合は、FACSや蛍光リーダーを用いて測定可能であるが、特定の細胞集団との結合が解析可能なFACSを選択した。H12-vesicleの蛍光標識はDiOC18で行った。DiOC18はリポソーム膜の脂質成分に結合するため、αIIbβ3結合部位であるH12への影響は最小限にとどめることができる。しかし、DiOC18標識H12-vesicleをFACSで解析した結果では、DiOC18の取り込みは均一に行われておらず、蛍光の強い集団と弱い集団の二峰性を呈していた。製造日時の異なるLot#903とLot#904を比較した結果でも、両者とも二峰性の染色パターンを示しており、蛍光標識を均一に行うのが困難であることを示している。今回の結果では、Lot#903とLot#904の平均蛍光強度はそれぞれ68.08、61.02であり、大きな違いはなかった。しかし、昨年度の脂質組成の異なるリポソームを標識した結果では、平均蛍光強度に大きな違いがあった。このようにリポソーム作成後に蛍光標識を行うと、その比活性をコントロールするのは困難と思われる。今後はリポソーム作成時に脂溶性の蛍光色素を予め一定の割合で含有させるなど、標識を均一に行う必要があると考えられる。

一過性発現細胞を用いた実験では、αIIbβ3発現量（蛍光強度）＞500の細胞集団へのH12-vesicle結合量（平均蛍光強度Geo Mean）を測定した。野生型αIIbβ3を発現した細胞では、H12-vesicleの結合はごく僅かであった。しかし活性化抗体PT25-2の存在下では、用量依存性に特異的結合の増加がみられた。Lot#903とLot#904の比較では、結合のKd値はそれぞれ2.75±0.54 mg/ml、2.45±0.39 mg/mlであり、Bmax値はそれぞれ278.7±27.7、302.0±23.3であった。この結果は、Lot#903とLot#904のαIIbβ3に対する結合親和性はほぼ同じであることを意味している。また細胞上のH12-vesicle結合部位数を反映するBmax値もほぼ同じ値であった。これらの結果からは、Lot#903とLot#904の機能に大きな差は無いと判断できる。一方、高活性型のQ595NTT変異体を発現した細胞では、PT25-2無しでも強い結合がみられた。Lot#903とLot#904のKd値はそれぞれ1.78±0.24 mg/ml、1.12±0.11 mg/ml、Bmax値はそれぞれ417.9±23.9、383.2±13.3であった。この結果は、Lot#903とLot#904はQ595NTT発現細胞上でほぼ同じ結合部位数を有するものの、結合親和性はLot#904が高いことを意味している。何故、野生型αIIbβ3を発現した細胞とQ595NTT発現細胞で異なる結果が得られたのであろうか？Kd値の比較ではQ595NTT発現細胞の方が常に低値であり、Q595NTTの方がPT25-2で活性化したαIIbβ3よりも高活性であることを示している。つまり、αIIbβ3の活性が高いほどH12-vesicleの親和性の違いが明らになると考えられる。野生型αIIbβ3発現細胞を用いた測定では、PT25-2の活性が鍵となるため、これが結果に影響を与える不確定要因となりうる。以上の結果から、Q595NTT発現細胞を用いた測定系が推奨される。

一過性発現細胞を用いた測定系では、測定毎に使用する細胞のαIIbβ3発現量は変化するため、測定日の違うデータを正確に比較するのは困難である。安定発現細胞を用いればαIIbβ3発現量は常に一定であるため、この問題は解決される。われわれは野生型αIIbβ3、Q595NTTを安定発現した細胞株を作成し、H12-vesicleの結合を調べた。期待に反して、これらの細胞に対す

る H12-vesicle の結合は非常に低く、信頼できるパラメーターを得ることはできなかった。原因は、一過性発現系で H12-vesicle 結合を調べる対象とした細胞群のαIIbβ3 発現量は 800-1000 であるのに対し、安定発現細胞株の発現量は野生型αIIbβ3#51 で 323.74、Q595NTT#48 で 153.42 と低いことに起因すると考えられる。野生型αIIbβ3#51 は二倍以上の発現量を有するにも拘わらず、Q595NTT#48 よりも H12-vesicle の結合量が低かった。この原因は、PT25-2 によるαIIbβ3 の活性化が Q595NTT よりも低いためと考えるのが妥当であろう。

一過性発現細胞、特に Q595NTT 変異体を発現した細胞と H12-vesicle の Kd 値は前年度 1.03±0.09 mg/ml と、本年度の Lot#904 の Kd 値と非常に近く、この測定系の再現性の高さがうかがえる。反面、野生型αIIbβ3 を PT25-2 で活性化する系では前年度 Kd 値 1.09±0.17 と、本年度の値とは大きく異なり再現性に乏しい。これは使用する PT25-2 の活性に結果が大きく左右されるためであろう。本年度の結果を総合すると、Q595NTT 変異体の一過性発現系が最も再現性の高い測定法と考えられる。安定発現系はαIIbβ3 の発現量が低く、H12-vesicle の結合解析には適さなかった。しかし、細胞を用いた測定系は細胞の状態、αIIbβ3 の発現量、αIIbβ3 の活性化、H12-vesicle の標識などの不確定要因が多く、測定系の再現性を確保する上で問題点となる。これらの要因を排除するためにも、無細胞測定系を用いるべきであろう。本年度は実施できなかったが、表面プラスモン共鳴を用いた測定系は最も実現性が高い。図１C に示したように、Q595NTT 変異体を固層化したセンサーチップに無標識の H12-vesicle を流すことによって、リアルタイムで結合測定が可能である。この方法では、前述した不確定要因もほとんどない。Q595NTT のソースとして今回樹立した安定細胞株を使用することができることもメリットである。今回、何故 Lot#903 と Lot#904 で異なる結合親和性を示したのかは不明である。今回実施した一過性細胞発現系と無細胞測定系を組み合わせることにより、H12-vesicle 製剤の品質管理に貢献できるだろう。

結論

高活性型αIIbβ3 発現した一過性発現細胞を用いることで、H12-vesicle 製剤の結合能を評価することが可能である。しかし、測定の再現性をさらに高めるためには、無細胞測定系の開発が必要と考えられる。

G. 研究発表

１論文発表：無し。

２学会発表: Kamata T, Handa M, Kawai Y, Ikeda Y, Aiso S: Separation of the two extracellular tails is required to propagate activation signals initiated in the cytoplasmic tails of αIIbβ3 integrin. The 23rd Congress of the International Society on Thrombosis and Haemostasis, Kyoto, Japan, July 23-28, 2011

H. 知的財産権の出願・登録：無し。

別添 5

Ⅲ．研究成果の刊行に関する一覧表

研究成果の刊行に関する一覧表

雑誌

発表者氏名	論文タイトル名	発表誌名	巻(号)	ページ	出版年
Suzuki, H., Okamura, Y., Ikeda, Y., Takeoka, S., Handa, M.	Ultrastructural analysis of thrombin-induced interaction between human platelets and liposomes carrying fibrinogen γ-chain dodecapeptide as a synthetic platelet substitute	*Thrombosis Research*	1285 (6)	552-559	2011
Yoshida H, Okamura Y, Watanabe N, Ikeda Y, Handa M.	Shear-dependent suppression of platelet thrombus formation by phosphodiesterase 3 inhibition requires low levels of concomitant Gs-coupled receptor stimulation	*Thromb Haemost*	105 (3)	487-495	2011
Tokutomi, K., Tagawa, K., Korenaga, M., Chiba, M., Asai, T., Watanabe, N., Takeoka, S., Handa, M., Ikeda, Y., Oku, N.	Decoration of fibrinogen γ-chain peptide on adenosine diphosphate-encapsulated liposomes enhances binding of the liposomes to activated platelets	*International Journal of Pharmaceutics*	407 (3)	151-157	2011
Taguchi K, Maruyama T, Otagiri M.	Pharmacokinetic properties of hemoglobin vesicles as a substitute for red blood cells	*Drug Metab Rev.*	43 (2)	362-373	2011
半田　誠	人工血小板	*脈管学*	51 (3)	333-378	2011

Ⅳ. 研究成果の刊行物・別冊

Thrombosis Research 128 (2011) 552–559

Contents lists available at ScienceDirect

Thrombosis Research

journal homepage: www.elsevier.com/locate/thromres

Regular Article

Ultrastructural analysis of thrombin-induced interaction between human platelets and liposomes carrying fibrinogen γ-chain dodecapeptide as a synthetic platelet substitute

Hidenori Suzuki [a,*], Yosuke Okamura [b], Yasuo Ikeda [b], Shinji Takeoka [b], Makoto Handa [c]

[a] Laboratory of Electron Microscopy, Tokyo Metropolitan Institute of Medical Science, Tokyo, Japan
[b] Department of Life Science and Medical Bioscience, Graduate School of Advanced Science and Engineering, Waseda University, TWIns, Tokyo, Japan
[c] Department of Transfusion Medicine & Cell Therapy, Keio University, Tokyo, Japan

ARTICLE INFO

Article history:
Received 13 May 2011
Received in revised form 15 July 2011
Accepted 15 July 2011
Available online 15 August 2011

Keywords:
Platelets
Platelet substitute
Liposomes
Dodecapeptide (H12)
Aggregation
Electron microscopy

ABSTRACT

Background: The dodecapeptide HHLGGAKQAGDV (H12) in the carboxy-terminus of the fibrinogen γ-chain is a specific binding site of the ligand for platelet GPIIb/IIIa complex. We have evaluated liposomes carrying fibrinogen γ-chain dodecapeptide as a synthetic platelet substitute.
Objectives: We examined the interaction between human platelets and H12-liposomes during thrombin-induced activation using flow cytometry and electron microscopy (EM).
Methods and results: After thrombin-activation, a remarkable time-dependent increase in binding of the H12-liposomes to platelets was found by flow cytometry. A large-sized swollen open canalicular system (OCS) was observed in the spheroidal platelets from 60 sec to 5 min after thrombin-activation, but intact H12-liposomes were not evident by conventional EM. Cryoultramicrotomy and immunogold staining with anti-H12 antibody were successful in identifying the liposomes; they appeared as small particles with a unit membrane around 0.2 to 0.4 μm in diameter, and gold labels representing H12 were distributed homogeneously on the surface. Abundant H12-liposomes were localized not only on the surface membrane but also in the lumen of the large-sized swollen OCS in the platelets at 60 sec after thrombin-activation. The formation of the large-sized swollen OCS was inhibited by pre-incubation with unbound H12, EDTA or anti-GPIIb/IIIa antibody. In thrombin-induced platelet aggregates we observed electron-transparent areas between adherent platelets, in which abundant H12-liposomes were distributed.
Conclusions: We demonstrate morphologically that H12-liposomes bind to thrombin-activated platelets and accumulate between adherent platelets like fibrinogen, leading to large-scale aggregation.

Introduction

Platelet transfusion plays an important role in prophylactic or therapeutic treatment for patients with thrombocytopenia caused by hematologic malignancies or intensive chemotherapy for solid tumors or as a result of surgical procedures and radiotherapy. However, due to the short storage life of platelets (4 days in Japan), the possibility of a shortage of platelets for transfusion has become a serious concern in our aging society. Furthermore, the risk of viral and bacterial infections being transmitted through transfusion is also a serious issue. To solve these problems, various platelet substitutes [1] have been developed, such as solubilized platelet membrane protein-conjugated liposomes (Plateletsome) [2], infusible platelet membranes (IPM) [3], fibrinogen-coated albumin microcapsules (Synthocyte) [4], red blood cells with bound fibrinogen [5], liposomes bearing fibrinogen [6], and arginine-glycine-aspartic acid (RGD) peptide-bound red blood cells (Thromboerythrocyte) [7].

We have developed platelet substitutes using polymerized albumin particles [8–11], phospholipid liposomes [12–15] and nanosheets [16] as biocompatible and biodegradable carriers and shown that carriers carrying recombinant fragments of platelet membrane proteins (rGPIbα [17,18] and rGPIa/IIa complex [19,20]) specifically interact with a surface that mimics the site of a bleeding injury, such as von Willebrand factor (VWF) and collagen immobilized on a surface under flow conditions *in vitro*. Moreover, we demonstrated that rGPIa/IIa-conjugated albumin particles reduced the tail bleeding time of thrombocytopenic mice [8]. These carriers have the ability to induce hemostasis; however, they cannot recruit flowing platelets to induce platelet aggregation.

Next we began the development of synthetic platelet substitutes based on a strategy of using polymerized albumin or liposomes (mean diameter, 0.22–0.26 μm for each) as a carrier vehicle and synthetic H12 peptides as a surface-coating ligand to target activated platelets

* Corresponding author at: Laboratory of Electron Microscopy, Tokyo Metropolitan Institute of Medical Science, 2-1-6 Kamikitazawa, Setagaya-ku, Tokyo 156–8506, Japan. Tel.: +81 3 5316 3100x1782; fax: +81 3 5316 3150.
E-mail address: suzuki-hd@igakuken.or.jp (H. Suzuki).

0049-3848/$ – see front matter © 2011 Elsevier Ltd. All rights reserved.
doi:10.1016/j.thromres.2011.07.031

[11,21–23]. It is well established that platelet aggregation is mediated via fibrinogen by bridging adjacent platelets through integrin αIIbβ3 (GPIIb/IIIa) in an activation-dependent manner [24–26]. Several sequences in fibrinogen have been designated as GPIIb/IIIa recognition sites: the RGD-based sequences ^{95}RGDF^{98} and ^{572}RGDS^{575} in the Aα chains; and ^{400}HHLGGAKQAGDV^{411} (H12, the fibrinogen γ-chain dodecapeptide) in the carboxy-terminus of the γ-chain [27–29]. Selection of the H12 peptide was derived from general observations that the interaction of H12 is highly specific to GPIIb/IIIa, whereas RGD related peptides are promiscuous with many integrins from various cell types [30]. In fact, H12-coated polymerized albumin and liposomes with polyethyleneglycol (PEG)-surface modifications show specific interactions with activated platelets and augmented effects on platelet thrombus formation onto collagen-immobilized surfaces under flow conditions *in vitro*, and prolonged hemostatic ability *in vivo* to correct bleeding time in a dose-dependent manner in a thrombocytopenic rat model [11,21–23].

However, we have only indirectly demonstrated the interaction between platelets and H12-particles *in vitro* or *in vivo*. In the present study, we carefully examined ultrastructural interactions between human platelets and H12-liposomes during thrombin-induced activation and aggregation, focusing on liposome localization using cryoultramicrotomy including immunogold staining. Although we failed to detect H12-liposomes using conventional electron microscopy, the application of cryoultramicrotomy has enabled us to identify these liposomes in both activated and aggregated platelets.

Materials and methods

Reagents

Cholesterol and 1,2-dipalmitoyl-*sn*-glycero-3-phosphatidylcholine (DPPC) were purchased from Nippon Fine Chemical (Osaka, Japan), and 1,2-distearoyl-*sn*-glycero-3-phosphatidyl- ethanolamine-*N*-[monomethoxypoly(ethyleneglycol)] (PEG-DSPE, 5.1 kDa) was from NOF (Tokyo, Japan). 1,5-Dihexadecyl-*N*-succinyl-L-glutamate (DHSG) and H12-PEG-Glu2C18, where fibrinogen γ-chain dodecapeptide (C-HHLGGAKQAGDV, Cys-H12) was conjugated to the end of the PEG-lipids, were synthesized. Carboxyfluoroscein (CF) was obtained from Acros Organics (Geel, Belgium). Polyvinylpyrrolidone, polyvinylalcohol (10 Da), prostaglandin E_1 (PGE_1), human thrombin and bovine serum albumin (BSA) were purchased from Sigma-Aldrich (St. Louis, MO, USA). Paraformaldehyde, glutaraldehyde, Epon, and uranyl acetate were obtained from TAAB Laboratories (Aldermaston, West Berkshire, UK). Rabbit antibody to H12 was synthesized by Oriental Yeast Co., Ltd. (Tokyo, Japan). PAC-1, a mouse anti-GPIIb/IIIa antibody, was purchased from Becton Dickinson (San Jose, CA, USA). Rabbit anti-human fibrinogen antibody and goat anti-rabbit IgG conjugated to 10- or 15-nm colloidal gold were obtained from Cappel Organon Teknika (West Chester, PA, USA) and BioCell Research Laboratories (Cardiff, UK), respectively. 2-[4-(2-Hydroxyethyl)-1-piperazinyl]ethanesulfonic acid (HEPES), ethylenediaminetetraacetic acid (EDTA) and other reagents were acquired from Wako Pure Chemical Industries, Ltd. (Osaka, Japan).

Preparation of H12-liposomes

The preparation was performed exactly as described previously [11,21–23]. Briefly, DPPC (100 mg), cholesterol (52.7 mg), DHSG (18.9 mg), PEG-DSPE (5.2 mg) and H12-PEG-Glu2C18 (4.7 mg) were dissolved in benzene and then freeze-dried (DPPC/cholesterol/DHSG/PEG-DSPE/H12-PEG-Glu2C18 = 5/5/1/0.033/0.033, by molar ratio). The resulting mixed lipids were hydrated with phosphate-buffered saline (PBS, pH 7.4, 5 mL) for 3 h at room temperature (RT) and extruded with membrane filters of pore size of 0.45 μm first and then with that of 0.22 μm (Durapore®; Millipore, Tokyo, Japan). For flow cytometric analysis, we also prepared the liposomes hydrated with a solution of CF in PBS (1 mM, 5 mL). The liposomes were washed with PBS by suspension and centrifugation (100,000×g, 30 min, 4 °C, twice), and the H12-liposomes and CF-labeled H12-liposomes were collected. We also prepared control liposomes (CF-labeled and unlabeled) in the absence of H12-PEG-Glu2C18 by the same procedure. The liposome diameter was analyzed using a dynamic light scattering method (N4 PLUS Particle Size Analyzer, Beckman-Coulter, Fullerton, CA, USA). The lipid concentration of liposome was quantified using a phospholipid test kit (Wako Pure Chemical Industries Ltd., Osaka, Japan).

Preparation of human washed platelets

Blood drawn from healthy volunteers was mixed with 10% volume of 3.8% sodium citrate. Blood collection was approved by the Committee of Tokyo Metropolitan Institute of Medical Science on the Ethics of Research in Human Experimentation. Platelet-rich plasma (PRP) was prepared by centrifugation of the blood (100×g, 15 min) at room temperature (RT). PRP was mixed with a 15% volume of acid-citrate-dextrose solution composed of 2.2% sodium citrate, 0.8% citric acid, and 2.2% glucose (ACD) containing 1 μM PGE_1. The suspension was centrifuged (2,200×g, 7 min, RT), and the plasma was replaced with a Ringer's-citrate-dextrose solution (RCD solution, composition: 0.76% citric acid, 0.09% glucose, 0.043% $MgCl_2$, 0.038% KCl, 0.60% NaCl, pH 6.5) containing 1 μM PGE_1. After the pellets were resuspended in the RCD solution, the suspension was centrifuged (2,200×g, 7 min, RT) and the concentrated platelets were resuspended at 1.0×10^5/μl in a Hepes-Tyrode buffer (H-T buffer, pH 7.4) containing 137 mM NaCl, 2.7 mM KCl, 0.4 mM NaH_2PO_4, 12 mM $NaHCO_3$, 1 mM $MgCl_2$, 22 mM $NaH_3C_6H_5O_7$, 5 mM HEPES, 0.35% BSA and 0.1% glucose. The platelet count was determined using an automated hematology analyzer (K-4500; Sysmex Co., Kobe, Japan).

Flow cytometry

After the addition of human thrombin (final concentration 0.1 U/ml) to mixtures of washed platelets (1.0×10^5/μl) and H12-CF-liposomes or control CF-liposomes (final concentration 3 mg/ml), the mixtures were gently shaken three times and allowed to stand without stirring for 30 sec, 60 sec, 5 min and 10 min at 37 °C. The incubation was terminated by adding an equal volume of 3% formaldehyde in PBS. After centrifugation, the platelets were resuspended in PBS. This washing procedure was repeated three times, after which platelets were gated according to their characteristic forward scatter versus side scatter, and 20,000 platelets were analyzed using a FACSCalibur flow cytometer (Nihon Becton Dickinson, Tokyo, Japan). The number of platelets bound to the H12-CF-liposomes or control CF-liposomes was quantified as a fraction of the fluorescent-positive platelets. Each experiment was performed at least three times.

Electron microscopy and immunogold electron microscopy

After the addition of thrombin to mixtures of washed platelets and H12-liposomes or control liposomes similar to flow cytometry, the mixtures were gently shaken three times and allowed to stand without stirring for 30 sec, 60 sec and 5 min at 37 °C, fixed with 0.2% glutaraldehyde in 0.1 M phosphate buffer (PB, pH 7.4). Part of the mixture of platelets and H12-liposomes was stirred for 60 sec after the addition of thrombin and fixed similarly above. To obtain control platelets before the addition of thrombin, washed platelets incubated with H12- or control liposomes alone were fixed in a manner similar to that described above. To block the function of GPIIb/IIIa, on the other hand, human platelets were pre-incubated with liposome-unbound H12 (0.5 mM), EDTA (5 mM) or the anti-GPIIb/IIIa antibody PAC-1 (10 μg/ml) for 60 sec before the addition of H12-liposomes and

thrombin. After fixation at 4 °C for 30 min, the fixed platelets were centrifuged at 2,200×g for 3 min and the platelet pellets were dissected into blocks of 1-mm cubes and divided into two samples: one for conventional electron microscopy and the other for cryoultramicrotomy including immunogold staining.

For electron microscopy, the samples were re-fixed with 2% glutaraldehyde in the same buffer at 4 °C for 30 min, washed with 0.1 M PB, post-fixed with 1% osmium tetroxide in same buffer at 4 °C for 60 min, dehydrated with a graded ethanol series, and embedded in Epon. After electron staining using uranyl acetate and lead citrate, ultrathin sections were examined with a JEM 1200EX transmission electron microscope (JEOL, Tokyo, Japan) at an accelerating voltage of 80 kV.

For cryoultramicrotomy and immunogold staining, the samples were processed according to the method of Tokuyasu [31] with minor modifications as previously described [32]. Briefly, the fixed platelets were rinsed with 0.1 M PB and PBS at 4 °C, then infused with 1 M sucrose in PBS for 60 min, 1.84 M sucrose in PBS for 2 h and then 1.84 M sucrose containing 20% polyvinylpyrrolidone in PBS overnight at 4 °C. After freezing in liquid nitrogen, ultrathin frozen sections were cut and were incubated with rabbit anti-H12 (1:5,000 dilution) or anti-human fibrinogen antibody (1:2,000 dilution) in PBS overnight at 4 °C. After rinsing with PBS five times, the sections were then incubated with goat anti-rabbit IgG coupled to 10 or 15-nm colloidal gold at a dilution of 1:100 for 60 min at RT. After rinsing with PBS three times and then distilled water (DW) five times, the sections were stained with 1% uranyl acetate, washed with DW, and then adsorption-stained with a mixture of 3% polyvinylalcohol and 0.3% uranyl acetate. The stained sections were examined with a JEM 1200EX electron microscope in a manner similar to that described above.

Results

Time-dependent increase in binding of H12-liposomes to thrombin-activated platelets

When thrombin was added to the mixture of human washed platelets and H12-liposomes, a significant time-dependent increase in binding of the liposomes to platelets was found by flow cytometry (Fig. 1). The binding of the liposomes to platelets had already begun by 30 sec and almost reached a plateau by 5 min after the addition of thrombin. The control liposomes, however, did not bind to platelets during the thrombin-induced activation.

Formation of a large-sized swollen open canalicular system (OCS) in platelets incubated with H12-liposomes after thrombin-induced activation

To assess the ultrastructural interaction of platelets with H12-liposomes after the addition of thrombin, ultrathin sections from Epon-embedded samples were subjected to transmission electron microscopy (Fig. 2). Before the addition of thrombin to the mixture of platelets and H12-liposomes, platelets had discoid forms, and organelles such as α-granules, dense granules, mitochondria, glycogen, and the open canalicular system (OCS) were well preserved in the platelet cytoplasm (Fig. 2A). Thirty seconds after the addition of thrombin, platelets had changed to spheroidal forms with pseudopodia,

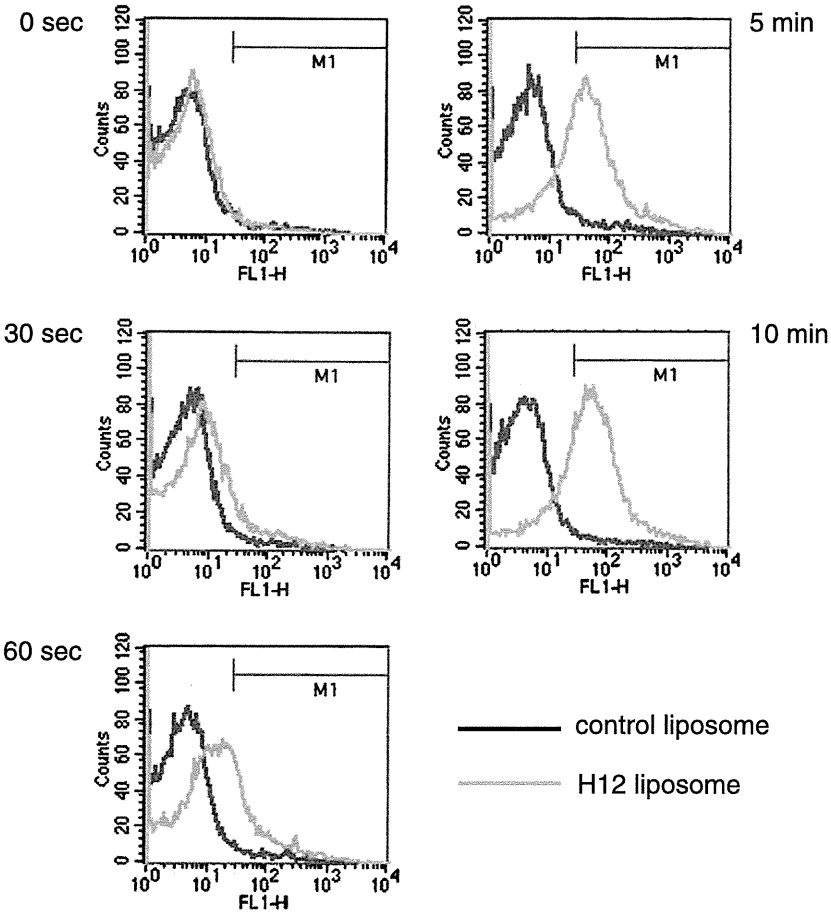

Fig. 1. Binding of H12-liposomes to thrombin-activated platelets by flow cytometry. After the addition of thrombin into mixtures of washed platelets and H12-CF-liposomes or control CF-liposomes, these mixtures were gently shaken three times and allowed to stand without stirring for 30 and 60 sec and 5 and 10 min at 37 °C, fixed with formaldehyde, washed with PBS, and analyzed using a FACSCalibur flow cytometer. The binding of the H12-CF-liposomes to platelets increased time-dependently, but that of control CF-liposomes did not change.

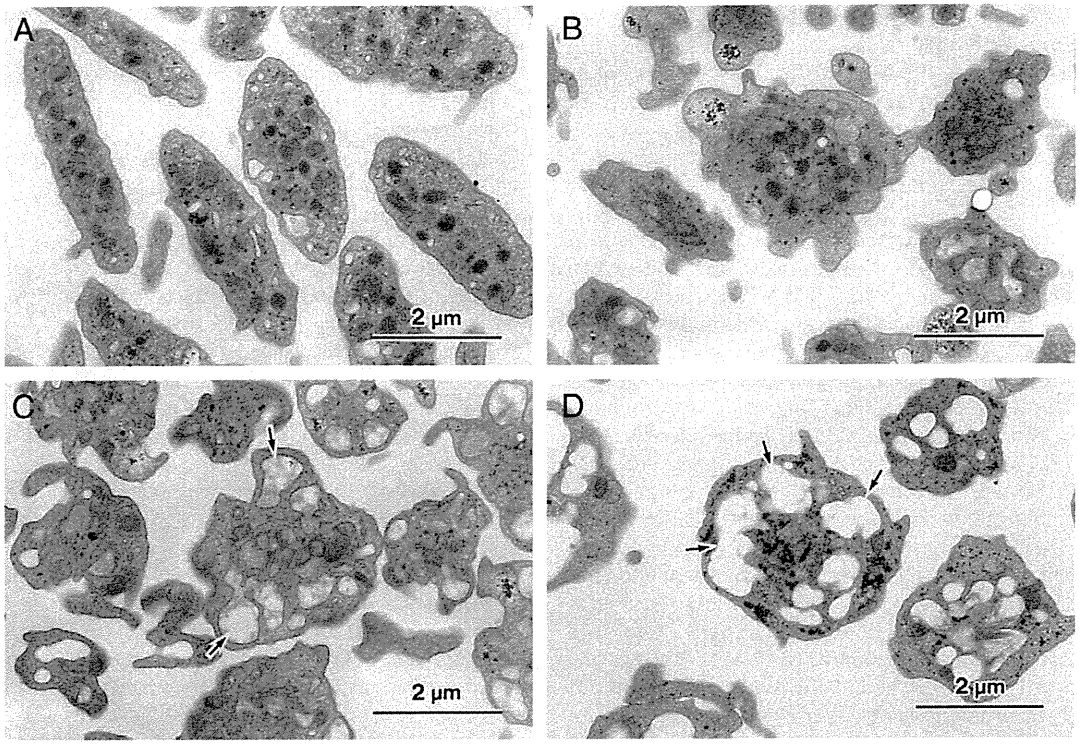

Fig. 2. Interaction of human platelets with H12-liposomes before and after the addition of thrombin. After the addition of thrombin, platelets were gently shaken three times and allowed to stand without stirring for 30 and 60 sec and 5 min at 37 °C, fixed with glutaraldehyde, post-fixed with osmium tetroxide, and embedded in Epon; ultrathin sections were then examined by transmission electron microscopy. (A) Before the addition of thrombin, platelets in the mixture with H12-liposomes have discoid forms containing cytoplasmic organelles such as α-granules, dense granules, mitochondria, glycogen, and the open canalicular system (OCS). (B) Thirty seconds after the addition of thrombin, platelets show spheroid forms with pseudopodia, and the centralization of granules can be seen. (C) At 60 sec, the OCS becomes expanded in the spheroidal platelets (arrows). (D) At 5 min, activated platelets have several large-sized swollen OCS (arrows), in which fuzzy and/or formless contents are present.

and the centralization of granules was observed (Fig. 2B). At 60 sec, the number of intact granules decreased; instead, several swollen OCS were observed in the spheroidal platelets (Fig. 2C). At 5 min, intact granules were no longer observed in the thrombin-activated platelets, indicating a release reaction had already occurred (Fig. 2D). The OCS was expanded to a size much larger than that of platelets at 60 sec after the addition of thrombin. There were several large-sized swollen OCS in the activated platelets whose longer axis was approximately equal to or greater than 1 μm. H12-liposomes, however, were not observed as intact forms during the activation. By careful inspection, fuzzy and/or formless contents were found to be present in the lumen of the large-sized swollen OCS. In contrast, the formation of large-sized swollen OCS could not be observed in the platelets incubated with control liposomes during the thrombin activation (data not shown).

Identification of H12-liposomes in thrombin-activated and aggregated platelets

To visualize H12-liposomes in the mixture with platelets before and after the addition of thrombin, ultrathin frozen sections from the samples were subjected to electron microscopy (Fig. 3). In the mixture of platelets and H12-liposomes before thrombin-activation, the liposomes were present independently from the platelets and were observed as electron-lucent small particles with unit membranes, around 0.2 to 0.4 μm in diameter (Fig. 3A). Through a combination of the immunogold method with an anti-H12 antibody, we were able to view H12 distributed homogeneously on the surface of the liposome (Fig. 3B), indicating that the method combining cryoultramicrotomy and immunogold staining was more effective at identifying liposomes than conventional electron microscopy methods.

Accordingly, the same methods were also used to analyze the interaction between platelets and H12-liposomes during thrombin-induced activation (Fig. 4–6). When thrombin was added into the mixture of platelets and H12-liposomes and the suspension was incubated without stirring from 30 sec to 5 min, the gold-labeled liposomes were identified not only on the exterior surface but also in the lumen of the large-sized swollen OCS in the platelets (Fig. 4). Interestingly, some H12-liposomes were localized along the membrane of the large-sized swollen OCS. In contrast, when the mixture of platelets

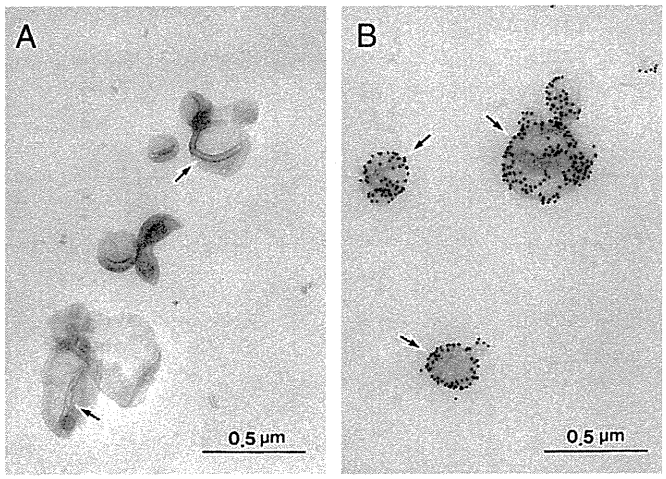

Fig. 3. Visualization of H12-liposomes by cryoultramicrotomy and immunogold staining. H12-liposomes in the mixture with platelets were fixed and frozen in liquid nitrogen, and ultrathin frozen sections were examined by electron microscopy before and after immunostaining with an anti-H12 antibody and gold-conjugated secondary antibody. (A) Liposomes show unilamellar small particles around 0.2 to 0.4 μm in diameter (arrows). (B) Abundant gold particles representing H12 are distributed homogeneously on the surface of the liposomes (arrows).

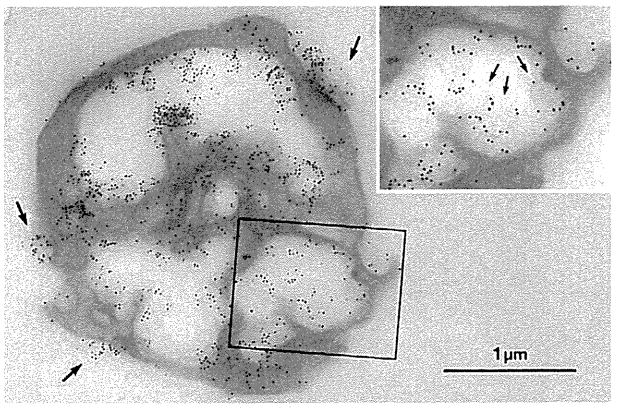

Fig. 4. Localization of H12-liposomes in the platelets activated by thrombin without stirring for 60 sec. The spheroidal platelet has several large-sized swollen OCS. Gold particles representing H12 are distributed not only on the exterior surface (arrows) but also in the lumen of the swollen OCS in the platelet. (Inset) At high-magnification, electron-lucent liposomes labeled with gold particles are visible along the membrane of the large-sized swollen OCS in the platelet (arrows).

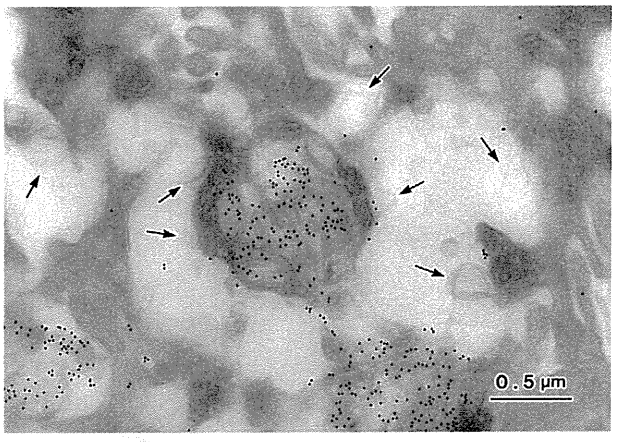

Fig. 6. Localization of fibrinogen in the platelet aggregates induced by thrombin for 60 sec. Many H12-liposomes with unit membranes are present in the electron-transparent areas between adherent platelets in the aggregates (arrows). Gold particles representing fibrinogen are densely distributed in the swollen or fused α-granules in the platelets discrete from the H12-liposomes.

and H12-liposomes was stirred for 60 sec after the addition of thrombin, extensive aggregates of platelets had formed (Fig. 5). The aggregates contained many electron-transparent areas between adherent platelets, ranging in diameter from around 1 μm to several μm, in which many H12-liposomes were identified (Fig. 5 inset). Although the ultrastructural appearance of the electron-transparent areas resembled that of the large-sized swollen OCS containing the liposomes in non-aggregated and activated platelets, their size was greater than that of the OCS. On the other hand, the localization of H12-liposomes in platelet aggregates differed from that of fibrinogen, as detected by immunogold staining (Fig. 6). Fibrinogen released from α-granules in platelets was densely localized in regions where granules appeared to be fused and at sites of discharge of the granule contents.

Inhibitory effect of antagonists to GPIIb/IIIa on the formation of the large-sized swollen OCS in platelets incubated with H12-liposomes after thrombin-induced activation

To assess the mechanism of formation of the large-sized swollen OCS in platelets incubated with H12-liposomes after thrombin-induced activation, liposome-unbound H12 and several antagonists to GPIIb/IIIa were subjected to ultrastructural analysis (Fig. 7). The control platelets in the mixture with H12-liposomes changed their form to spheroids and contained several large-sized swollen OCS 5 min after the addition of thrombin (Fig. 7A). In contrast, when the mixture of platelets and H12-liposomes was pre-incubated with liposome-unbound H12 (Fig. 7B), EDTA (Fig. 7C) or the anti-GPIIb/IIIa antibody PAC-1 (Fig. 7D) for 60 sec at 37 °C, the formation of the large-sized swollen OCS at 5 min after the addition of thrombin was inhibited completely. Especially in the platelets pre-incubated with liposome-unbound H12, not only the formation of the large-sized swollen OCS but also the release reaction of granules was inhibited after the addition of thrombin.

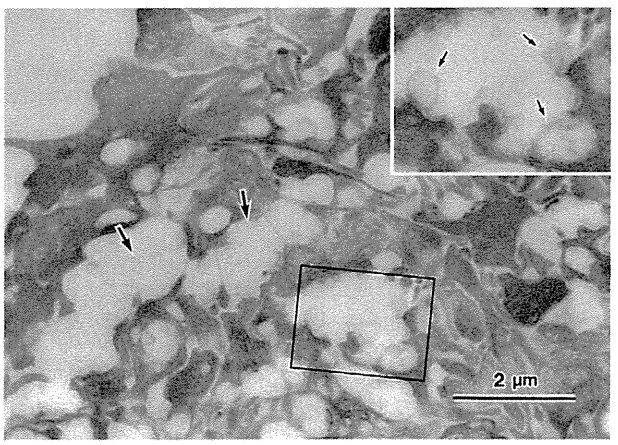

Fig. 5. Localization of H12-liposomes in the platelet aggregates induced by thrombin for 60 sec. Large aggregates have formed and many platelets have been degranulated. Electron-transparent areas between adherent platelets are widespread in the aggregates (arrows). (Inset) At high-magnification, H12-liposomes can be observed on the membrane of platelets in the electron-transparent areas (arrows).

Discussion

We have previously confirmed that H12-coated microparticles such as liposomes, latex, and nanosheets show specific interaction with activated platelets and augmented effects on platelet thrombus formation onto collagen-immobilized surfaces under flow conditions *in vitro*, and prolonged hemostatic ability *in vivo* to correct bleeding time in a dose-dependent manner in a thrombocytopenic rat model [11,16,21–23]. These findings indicated that H12 on the surface of the particles reproduced the ability to bind GPIIb/IIIa on the activated platelet, leading to adhesion and aggregation at the site of vascular injury [33]. Our purpose in this study was to visualize the specific interaction between human platelets and H12-liposomes during thrombin-induced activation using flow cytometry and electron microscopy.

Our flow cytometry results suggest that many H12-liposomes should be associated with the surface of the thrombin-activated platelets, and that this should be visible through electron microscopy. In contrast to our expectation, however, we could not identify H12-liposomes associated with platelets before and after the addition of thrombin in the sections of Epon-embedded sample using conventional electron microscopy. Instead, we observed the formation of large-sized swollen OCS, 1 μm in diameter or larger, in the spheroidal platelets from 60 sec to 5 min after the addition of thrombin. Furthermore, hazy and/or formless contents were present in the lumen of the OCS. Swollen OCS is observed commonly during the platelet release reaction; its size is usually about 0.5 μm in diameter [32,34,35]. It is well known that actin assembly induced by an increase of intracellular $[Ca^{2+}]$ and activation of protein kinase C in response to several agonists results in the platelet release reaction as follows: α-granules fuse with each other and the membrane of the OCS, resulting in the formation of the swollen OCS, and causing the intra-granule contents to be compressed so as to flow through the lumen of the OCS

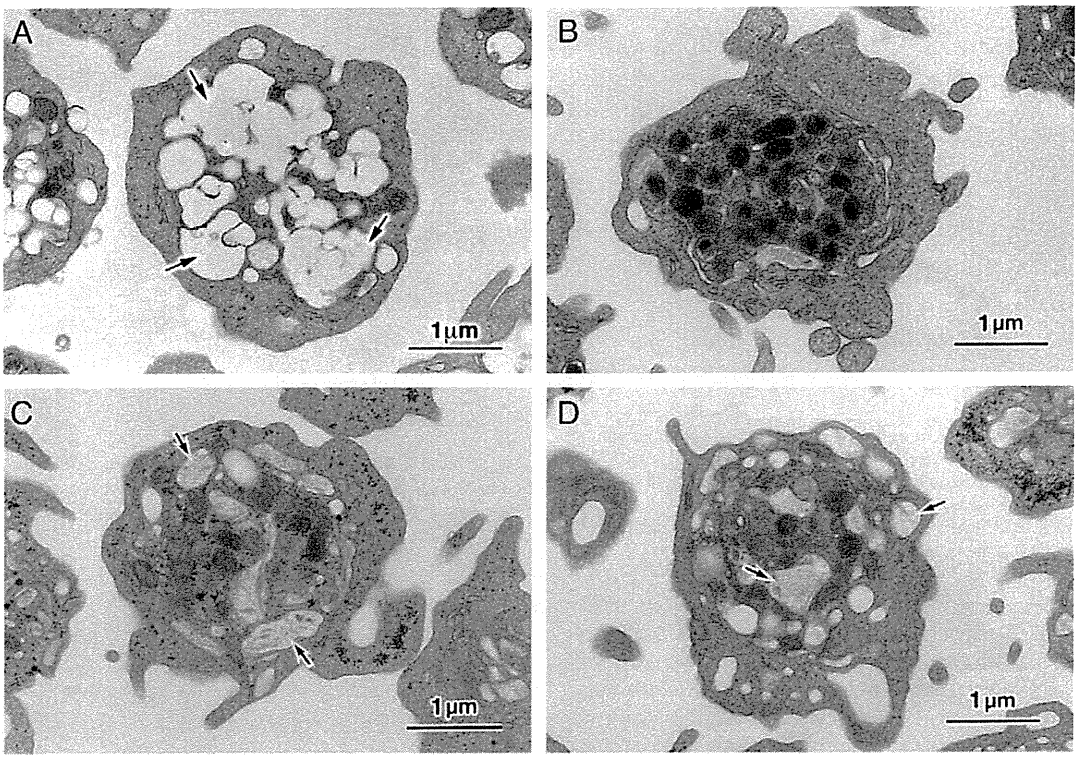

Fig. 7. Effect of antagonists to GPIIb/IIIa on the formation of the large-sized swollen OCS in platelets incubated with H12-liposomes after thrombin-induced activation. The mixture of platelets with H12-liposomes was pre-incubated with liposome-unbound H12, EDTA or the anti-GPIIb/IIIa antibody PAC-1 for 60 sec at 37 °C, activated with thrombin for 5 min without stirring, fixed and viewed by conventional electron microscopy. (A) Control platelets in the mixture with H12-liposomes appear as spheroid forms with several large-sized swollen OCS at 5 min after the addition of thrombin (arrows). (B) When the mixture of platelets and H12-liposomes was pre-incubated with liposome-unbound H12, the platelets have spheroid forms with pseudopodia, and the centralization of granules can be seen after thrombin activation, though the swollen OCS cannot. (C) The platelets pre-incubated with EDTA appear as spheroid forms similar to H12-pre-incubated cells after thrombin activation. Some α-granules are fusing with the membrane of the OCS, resulting in the release reaction of granules in the platelets. On the other hand, the lumen size of the OCS is relatively normal, and there is no large-scale swelling (arrows). (D) After thrombin activation, the platelets pre-incubated with PAC-1 are striking similar in shape to the EDTA-pre-incubated ones. The release of storage granules is observed in the platelets (arrows), but the large-sized swollen OCS is not.

to the exterior of the platelets. Moreover, recent studies have suggested that soluble NSF attachment protein receptors (SNARE) proteins such as syntaxin, SNAP-23 and VAMP and Rab proteins participate in the α-granule fusion and the formation of swollen OCS [36,37]. In the present study, using ultrathin frozen sections and immunogold electron microscopy, we have succeeded in visualizing H12-liposomes localized not only on the surface membrane but also in the lumen of the swollen OCS in the platelets from 60 sec to 5 min after the addition of thrombin. The swollen OCS containing H12-liposomes in the platelets of ultrathin frozen sections expanded greatly, similar to the platelet OCS in the sections of Epon-embedded sample. We also observed that the large-sized swollen OCS failed to form in the thrombin-activated platelets with control liposomes. Taken together, these observations lead to the conclusion that the large-sized swollen OCS is formed after specific interaction between platelets and H12-liposomes by the following pathway: H12-liposomes bind to the surfaces of spheroidal platelets after thrombin stimulation, and a fraction of the liposomes redistribute into the lumen of the OCS in the platelets, resulting in the formation of the large-sized swollen OCS in the cells. We confirmed that the formation of the large-sized swollen OCS was a GPIIb/IIIa-mediated interaction, because it was completely inhibited by pre-incubation with liposome-unbound H12, EDTA or the anti-GPIIb/IIIa antibody PAC1. However, the physiological role of the redistribution of H12-liposomes from the platelet surface to the OCS and the formation of the large-sized OCS remains unknown, although several investigators have reported that platelets have the ability to take up small particles such as cationized ferritin, latex, bacteria and viruses [38–40] into the lumen of the OCS. Some electron microscopic studies using cytochemical methods have also demonstrated that these small particles were eventually internalized into the platelet cytoplasm from the OCS by phagocytosis [38,40]. Whether the above-mentioned redistribution of H12-liposomes participates in platelet phagocytosis remains to be determined. The hazy and/or formless contents present in the lumen of the large-sized swollen OCS seemed to be the wreckage of the H12-liposome, which had been dissolved and broken down by the ethyl alcohol used for dehydration during sample preparation.

In the thrombin-induced aggregates, H12-liposomes were found to localize in the electron-transparent areas between adherent platelets in the aggregates. The large-sized swollen OCS containing H12-liposomes observed in non-aggregated platelets may be formed in each platelet even in the aggregates. Although it may appear that the electron-transparent areas were just as small as the OCS, we could not identify the OCS containing H12-liposomes in the aggregated platelets due to difficulties in distinguishing between the demarcated boundaries of each platelet in the aggregates. At any rate, these findings indicate that H12-liposomes bind to stimulated platelets and are incorporated between adherent platelets in the aggregates. The process of platelet aggregation is known to be regulated by the activation of GPIIb/IIIa and its subsequent binding of fibrinogen or other adhesive proteins [24–30]. When washed human platelets in the presence of exogenous fibrinogen were stimulated by ADP or thrombin, fibrinogen was found to localize between entire adherent platelets in the aggregates [35,41]. In the present study, although the localization of H12-liposomes differed from that of fibrinogen released from α-granules in the thrombin-induced aggregates, the localization of liposomes seems to resemble that of the exogenous fibrinogen in the ADP- or thrombin-induced aggregation, suggesting that H12-liposomes behave like fibrinogen by bridging adjacent platelets through GPIIb/IIIa activation after the addition of thrombin,

leading to the formation of the aggregates consisting of platelets and the liposomes. H12-liposomes have two advantages over fibrinogen in terms of their participation in the platelet aggregates. The first is that the modified H12 on the surface of liposomes is specifically bound to the activated GPIIb/IIIa on the surface of the platelets. Several sequences in fibrinogen have been designated as GPIIb/IIIa recognition sites, including two RGD-based sequences in the Aα chains and H12 in the carboxy-terminus of the γ-chain [27–29]. Selection of the H12 peptide was based on general observations that the interaction of H12 is highly specific to GPIIb/IIIa, whereas RGD-related peptides are promiscuous with many integrins from various cell types [30]. Thus, it is assumed that the binding ability of H12-liposomes to activated GPIIb/IIIa on the platelet surface is stronger than that of fibrinogen. The second advantage of H12-liposomes is that they have a diameter of about 0.3 μm. It is assumed that due to their large size compared to that of fibrinogen molecules, H12-liposomes are capable of forming large aggregates in combination with only a small number of platelets. In fact, even in a thrombocytopenic rat model, H12-liposomes reduced bleeding time in a dose-dependent manner, suggesting that the liposomes interact with small numbers of platelets and form big aggregates at sites of vascular injury [22,23].

In conclusion, we have clarified the interaction between platelets and H12-liposomes during thrombin-induced activation using flow cytometry and electron microscopy. In a previous study, Okamura et al. succeeded in visualizing the specific accumulation of H12-liposomes at a site of vascular injury using iopamidol encapsulation and computed tomography observation, and undertook semiquantitative analyses of the H12-liposomes accumulated at the injured site [33]. They also generated schematic images of the accumulation mechanism of H12-liposomes at endothelial injury sites. Our present finding, namely, that H12-liposomes were localized abundantly between adherent platelets in the thrombin-induced aggregates, strongly supports the theory that the liposomes could participate in hemostasis by accumulating specifically in platelet aggregates at the site of bleeding. H12-liposomes appear to require endogenous platelets to work, and thus may not be sufficiently effective when administered to patients with significant thrombocytopenia. Yet H12-liposomes may be useful for the treatment of bleeding in patients with qualitative platelet disorders, such as storage pool deficiency. Further study is needed under conditions simulating various clinical settings to establish potential indications in platelet transfusion.

Disclosure of conflict of interests

The authors state that they have no conflict of interest.

Acknowledgements

This work was supported in part by Health and Labor Sciences Research Grants (Research on Public Essential Drugs and Medical Devices, H. Suzuki, Y. Ikeda, S. Takeoka and M. Handa) from the Ministry of Health, Labour and Welfare, Japan.

References

[1] Blajchman MA. Substitutes and alternatives to platelet transfusions in thrombocytopenic patients. J Thromb Haemost 2003;1:1637–41.
[2] Rybak M, Renzulli LA. A liposome based platelet substitute, the plateletsome, with hemostatic efficacy. Biomater Artif Cells Immobilization Biotechnol 1993;21:108–18.
[3] Graham SS, Gonchoroff NJ, Miller JL. Infusible platelet membranes retain partial functionality of the platelet GPIb/IX/V receptor complex. Am J Clin Pathol 2001;115:144–7.
[4] Levi M, Friedrich PW, Middleton S, De Groot PG, Wu YP, Harris R, et al. Fibrinogen-coated albumin microcapsules reduce bleeding in severely thrombocytopenic rabbits. Nat Med 1999;5:107–11.
[5] Agam G, Livine AA. Erythrocytes with covalently bound fibrinogen as a cellular replacement for the treatment of thrombocytopenia. Eur J Clin Invest 1992;22:105–12.
[6] Casals E, Verdaguer A, Tonda R, Galan A, Escolar G, Estelrich J. Atomic force microscopy of liposomes bearing fibrinogen. Bioconjugate Chem 2003;14:593–600.
[7] Coller BS, Springer KT, Beer JH, Mohandas N, Scudder LE, Norton KJ, et al. Thromboerythrocytes. In vitro studies of a potential autologous, semi-artificial alternative to platelet transfusion. J Clin Invest 1992;89:546–55.
[8] Teramura Y, Okamura Y, Takeoka S, Tsuchiyama H, Narumi H, Kainoh M, et al. Hemostatic effects of polymerized albumin particles bearing rGPIa/IIa in thrombocytopenic mice. Biochem Biophys Res Commun 2003;306:256–60.
[9] Takeoka S, Teramura Y, Okamura Y, Handa M, Ikeda Y, Tsuchida E. Fibrinogen-conjugated albumin polymers and their interaction with platelets under flow conditions. Biomacromolecules 2001;2:1192–7.
[10] Takeoka S, Teramura Y, Ohkawa H, Ikeda Y, Tsuchida E. Conjugation of von Willebrand factor-binding domain of platelet glycoprotein Ibα to size-controlled albumin microspheres. Biomacromolecules 2000;1:290–5.
[11] Okamura Y, Takeoka S, Teramura Y, Maruyama H, Tsuchida E, Handa M, et al. Hemostatic effects of fibrinogen-γ chain dodecapeptide-conjugated polymerized albumin particles *in vitro* and *in vivo*. Transfusion 2005;45:1221–8.
[12] Takeoka S, Teramura Y, Okamura Y, Tsuchida E, Handa M, Ikeda Y. Rolling properties of rGPIbα-conjugated phospholipid vesicles with different membrane flexibilities on vWf surface under flow conditions. Biochem Biophys Res Commun 2002;296:765–70.
[13] Kitaguchi T, Murata M, Iijima K, Kamide K, Imagawa T, Ikeda Y. Characterization of liposomes carrying von Willebrand factor-binding domain of platelet glycoprotein Ibα: A potential substitute for platelet transfusion. Biochem Biophys Res Commun 1999;261:784–9.
[14] Nishiya T, Murata M, Handa M, Ikeda Y. Targetting of liposomes carrying recombinant fragments of platelet membrane glycoprotein Ibα to immobilized von Willebrand factor under flow conditions. Biochem Biophys Res Commun 2000;270:755–60.
[15] Nishiya T, Kainoh M, Murata M, Handa M, Ikeda Y. Reconstitution of adhesive properties of human platelets in liposomes carrying both recombinant glycoproteins Ia/IIa and Ibα under flow conditions: specific synergy of receptor-ligand interactions. Blood 2002;100:136–42.
[16] Okamura Y, Fukui Y, Kabata K, Suzuki H, Handa M, Ikeda Y, et al. Novel platelet substitutes: disk-shaped biodegradable nanosheets and their enhanced effects on platelet aggregation. Bioconjug Chem 2009;20:1958–65.
[17] Murata M, Ware J, Ruggeri ZM. Sitedirected mutagenesis of a soluble recombinant fragment of platelet glycoprotein Ibα demonstrating negatively charged residues involved in von Willebrand factor binding. J Biol Chem 1991;266:15474–80.
[18] Marchese P, Saldivar E, Ware J, Ruggeri ZM. Adhesive properties of the isolated amino-terminal domain of platelet glycoprotein Ibα in a flow field. Proc Natl Acad Sci USA 1999;96:7837–42.
[19] Sixma JJ, van Zanten GH, Huizinga EG, van der Plas RM, Verkley M, Wu YP, et al. Platelet adhesion to collagen: An update. Thromb Haemostasis 1997;78:434–8.
[20] Santro SA, Zutter MM. The α2β1 integrin: a collagen receptor on platelets and other cells. Thromb Haemost 1995;74:813–21.
[21] Takeoka S, Okamura Y, Teramura Y, Watanabe N, Suzuki H, Tsuchida E, et al. Function of fibrinogen γ-chain dodecapeptide-conjugated latex beads under flow. Biochem Biophys Res Commun 2003;312:773–9.
[22] Okamura Y, Maekawa I, Teramura Y, Maruyama H, Handa H, Ikeda Y, et al. Hemostatic effects of phospholipid vesicles carrying fibrinogen γ-chain dodecapeptide *in vitro* and *in vivo*. Bioconjug Chem 2005;16:1589–96.
[23] Okamura Y, Fujie T, Maruyama H, Handa M, Ikeda Y, Takeoka S. Prolonged hemostatic ability of poly(ethylene glycol)-modified polymerized albumin particles carrying fibrinogen γ-chain dodecapeptide. Transfusion 2007;47:1254–62.
[24] Mustard JF, Packham MA, Kinlough-Rathbone RL. Fibrinogen and ADP-induced platelet aggregation. Blood 1978;52:453–66.
[25] Nachman RL, Leung LL. Complex formation of platelet membrane glycoproteins IIb and IIIa with fibrinogen. J Clin Invest 1982;69:263–9.
[26] Shattil SJ, Hoxie JA, Cunningham M, Brass LF. Changes in the platelet membrane glycoprotein IIb-IIIa complex during platelet activation. J Biol Chem 1985;260:11107–14.
[27] Hawiger J, Kloczewiak M, Bednarek MA, Timmons S. Platelet receptor recognition domains on the α chain of human fibrinogen: structure-function analysis. Biochemistry 1989;28:2909–14.
[28] Kloczewiak M, Timmons S, Hawiger J. Localization of a site interacting with human platelet receptor on carboxy-terminal segment of human fibrinogen γ chain. Biochem Biophys Res Commun 1982;107:181–7.
[29] Kloczewiak M, Timmons S, Lukas TJ, Hawiger J. Platelet receptor recognition site on human fibrinogen. Synthesis and structure-function relationship of peptides corresponding to the carboxy-terminal segment of the γ chain. Biochemistry 1982;23:1767–74.
[30] Phillips DR, Charo IF, Scarborough RM. GPIIb-IIIa: the responsive integrin. Cell 1991;65:359–62.
[31] Tokuyasu KT. Use of poly(vinylpyrrolidone) and poly(vinyl alcohol) for cryoultramicrotomy. Histochem J 1989;21:163–71.
[32] Suzuki H, Yamazaki Y, Tanoue K. Immunocytochemical aspects of platelet membrane glycoproteins and adhesive proteins during activation. Progr Histochem Cytochem 1996;30:1–109.
[33] Okamura Y, Eto K, Maruyama H, Handa M, Ikeda Y, Takeoka S. Visualization of liposomes carrying fibrinogen γ-chain dodecapeptide accumulated to sites of vascular injury using computed tomography. Nanomedicine 2010;6:391–6.
[34] White JG. Electron microscopic studies of platelet secretion. Progr Hemost Thromb 1974;2:49–98.
[35] Suzuki H, Kinlough-Rathbone RL, Packham MA, Tanoue K, Yamazaki H, Mustard JF. Immunocytochemical localization of fibrinogen during thrombin-induced aggregation of washed human platelets. Blood 1988;71:1310–20.

[36] Ren Q, Ye S, Whiteheart SW. The platelet release reaction: just when you thought platelet secretion was simple. Curr Opin Hematol 2008;15:537–41.
[37] Blair P, Flaumenhaft R. Platelet α-granules: Basic biology and clinical correlates. Blood Rev 2009;23:177–89.
[38] Youssefian T, Drouin A, Massé JM, Guichard J, Cramer EM. Host defense role of platelets: Engulfment of HIV and *Staphylococcus aureus* occurs in a specific subcellar component and is enhances by platelet activation. Blood 2002;99:4021–9.
[39] White JG. Why human platelets fail to kill bacteria. Platelets 2006;17:191–200.
[40] Li X, Iwai T, Nakamura H, Inoue Y, Chen Y, Umeda M, et al. An ultrastructural study of *Porphyromonas gingivalis*-induced platelet aggregation. Thromb Res 2008;122: 810–9.
[41] Suzuki H, Kinlough-Rathbone RL, Packham MA, Tanoue K, Yamazaki H, Mustard JF. Immunocytochemical localization of fibrinogen on washed human platelets. Lack of requirement for fibrinogen during adenosine dephosphate induced responses, and enhanced fibrinogen binding in a medium with low calcium levels. Blood 1988;71:850–60.

Shear-dependent suppression of platelet thrombus formation by phosphodiesterase 3 inhibition requires low levels of concomitant Gs-coupled receptor stimulation

Hideo Yoshida[1,3]; Yosuke Okamura[2,3]; Naohide Watanabe[3]; Yasuo Ikeda[2]; Makoto Handa[3]

[1]Tokyo New Drug Research Laboratories, Kowa Company, Ltd., Tokyo, Japan; [2]Department of Life Science and Medical Bioscience, Graduate School of Advanced Science and Engineering, Waseda University, Tokyo, Japan; [3]Departments of Transfusion Medicine & Cell Therapy, School of Medicine, Keio University, Tokyo, Japan

Summary

Phosphodiesterase (PDE)3 inhibitors exert potent antiplatelet effects through maintaining elevated intracellular cyclic adenosine monophosphate levels, but do not prolong bleeding time. To resolve this discrepancy, we hypothesised that PDE3 inhibitors effectively suppress shear-induced platelet thrombus formation initiated by the interaction of the platelet receptor GPIb/V/IX with its ligand, von Willebrand factor (VWF), since arterial thrombosis is more dependent on shear stress as compared with haemostatic plug formation. To test the hypothesis, we compared the *in vitro* effects of K-134 (a PDE3 inhibitor), tirofiban (a GPIIb/IIIa inhibitor) and acetylsalicylic acid (ASA) on ristocetin-induced platelet aggregation and platelet thrombus formation on VWF or collagen surfaces under flow conditions. K-134 inhibited GPIIb/IIIa-dependent platelet aggregation to the same extent as tirofiban and more potently than ASA. Likewise, K-134 and tirofiban effectively inhibited stable platelet thrombus formation (platelet firm adhesion and subsequent aggregation) on the VWF or collagen surface under high shear, but ASA only inhibited aggregation. Notably, inhibition by K-134 became evident only when a low concentration of PGE1 was present. These inhibitors did not block shear-induced initial platelet contact with VWF via GPIb/V/IX. In contrast, under low shear, the inhibitory effects of K-134 on platelet aggregation on the collagen surface were lower than tirofiban or ASA. The observed shear-dependent suppression of platelet thrombus formation by PDE3 inhibitor in the presence of low levels of adenylate cyclase stimulator may contribute to high therapeutic benefit with low risk of bleeding.

Keywords

Phosphodiesterase 3 inhibitor, GPIb/V/IX, VWF, shear-induced platelet thrombus formation, PGE1

Correspondence to:
Makoto Handa
Department of Transfusion Medicine & Cell Therapy
School of Medicine, Keio University
35 Shinanomachi, Shinjuku-ku, Tokyo 160–8582, Japan
Tel.: +81 3 3353 1211 (ext. 62113), Fax +81 3 3353 9706
E-mail: mhanda@sc.itc.keio.ac.jp

Received: July 10, 2010
Accepted after major revision: November 25, 2010
Prepublished online: December 6, 2010
doi:10.1160/TH10-07-0439
Thromb Haemost 2011; 105: 487–495

Introduction

In platelets, cyclic adenosine monophosphate (cAMP) is a versatile negative regulator of key signalling pathways including Ca^{2+} mobilisation and integrin αIIbβ3 (glycoprotein (GP)IIb/IIIa) activation, virtually through serine/threonine phosphorylation by the cAMP-dependent protein kinase (PK)A. The cAMP is synthesised from adenosine triphosphate (ATP) by adenylate cyclase (AC), activated by Gs-coupled receptor stimulation with endogenous agonists such as prostaglandin (PG)I2 (also known as prostacyclin) or adenosine, and is degraded to 5'-AMP by cyclic guanosine monophosphate (cGMP)-inhibited cAMP phosphodiesterase (PDE)3. As a result, cAMP concentrations in platelets are regulated by the activity balance between AC and PDE3 (1). In fact, a prominent functional synergy exists *in vitro* and *ex vivo* between AC stimulation (e.g. by the PGI2 analogue PGE1) and PDE3 inhibition (e.g. by the PDE3 inhibitor cilostazol) to suppress platelet activation (1).

Cilostazol is the only PDE3 inhibitor to date approved for clinical use to manage intermittent claudication in patients with peripheral arterial disease (PAD) (2), and has been shown to inhibit agonist-induced human platelet aggregation *ex vivo* as effectively as the cyclooxygenase inhibitor acetylsalicylic acid (ASA) and the P2Y12 inhibitor clopidogrel (3). Although use of ASA or clopidogrel is complicated by an increased risk of bleeding, cilostazol does not prolong human bleeding time (3, 4), and the risk of haemorrhage associated with treatment is quite low (5, 6). To clarify this discrepancy, we hypothesised that PDE3 inhibitors suppress platelet thrombus formation in a shear-dependent manner, since pathological thrombus at injured arterioles or stenosed arteries is more dependent on high shear stress than physiological haemostatic plug formation. Thrombus formation on von Willebrand factor (VWF) and collagen surfaces under high shear requires association of platelet GPIb/V/IX with the A1 domain of VWF (7, 8), and GPIb/V/IX engagement itself activates GPIIb/IIIa independently of other receptors (9). Conversely, under low shear, direct platelet binding to collagen via GPVI, and platelet-to-platelet crosslinking via GPIIb/IIIa and fibrinogen are functionally significant in thrombus formation on collagen (10, 11), whereas GPIb/V/IX is not necessarily required (8).